Reaction of Nitric Oxide and Ozone in Cryogenic Matrices. Quantum-Mechanical Tunneling and Vibrational Enhancement

Heinz Frei and George C. Pimentel*

Chemistry Department, University of California, Berkeley, California 94720 *(Received: July 14, 1981; In Final Form: August 3, 1981)*

The cryogenic reaction between nitric oxide and ozone has been reexamined in solid nitrogen, argon, and krypton matrices at 6-20 K. In the absence of light, the kinetics of the growth of NO_2 is close to first order but is more accurately represented by a superposition of two first-order processes. In a nitrogen matrix, $NO/O_3/N_2 = 1:1:100$, the closest first-order rate constant is 0.1 h^{-1}, and it is virtually temperature independent (6-16 K) provided the kinetics are measured at a temperature below the deposition temperature. The absence of temperature dependence and a significant ^{18}O isotope effect on the rate indicate that heavy-atom tunneling is involved. When the NO in $NO\cdot O_3$ nearest-neighbor pairs is vibrationally excited with a CO laser, the rate constant increases linearly with the laser power. This shows that the rate is enhanced in the cryogenic environment by NO vibrational excitation (photon energy, 5.4 kcal mol^{-1}) in a one-photon process with low quantum yield.

Introduction

The kinetics of the reaction between nitric oxide and ozone has been extensively studied[1-12] since the work of Thrush and co-workers[1] revealed the presence of two reaction channels with different activation energies, 4.18 and 2.33 kcal mol^{-1}, respectively. This novel feature enhances the theoretical interest in this important atmospheric reaction and accounts for the continued attention which it receives. Recent work confirms the existence of the second, low activation energy channel and suggests that reaction of NO in its lower, $X(^2\Pi_{1/2})$ state produces vibrationally excited NO_2 in its ground electronic state.[3,4] The second channel, which produces electronically excited NO_2 $B(^2B_2)$ is attributed to NO in the $X(^2\Pi_{3/2})$ state. However, the molecular-beam work of Anderson et al.[9] and of Van den Ende and Stolte[10] calls this into question.

The rate enhancement caused by selective vibrational excitation of each reactant has also been measured.[6-8] These successes stimulated a study of this reaction in cryogenic matrices in which only the ground state of NO need be considered[12] (hereafter, this study will be called I). Surprisingly, reaction proceeded at 12 K even when the sample was completely enclosed by a 50 K radiation shield. The temperature dependence of the rate indicated an apparent activation energy near 106 cal mol^{-1}, the ^{18}O isotope effect did not seem to support a tunneling mechanism, and exposure of the sample to the infrared radiation from a conventional Nernst glower had no measurable effect on the reaction rate. Without a clear-cut explanation of these unexpected results, Lucas and Pimentel[12] focus attention on the possibility that they are to be explained by the configurational constraints placed on the reactants and the activated complex by the matrix environment.

We describe here a fresh attempt to elucidate the mechanism of the dark, cryogenic reaction by using a spectrometer of much higher sensitivity and resolution. Then the effect of selective vibrational excitation was reinvestigated by using much more intense infrared laser sources.

Experimental Section

The cryogenic, laser, and spectroscopic equipment as well as the deposition and laser irradiation technique have been described fully in a preceding paper[13] (hereafter, ref 13 will be called II). Separate NO and O_3 mixtures in nitrogen, argon, or krypton were simultaneously deposited from dual jets onto a cold CsI window. Deposition time was 1 h at a total rate of 1 mmol h^{-1}. In some experiments, deposition was conducted at a fixed temperature (±1 K) between 10 and 20 K and then the sample was cooled to a lower temperature at which the cryogenic reaction was studied. In these cases, the deposited sample was held at the lower temperature for 15 min before the first spectrum was taken.

Reaction kinetics was followed by infrared spectroscopy using a FT IR spectrometer (Nicolet, Model 7199). Spectra were recorded over a period of 10 min once every 90 min at a resolution of 0.24 cm^{-1} and with frequency accuracy better than 0.1 cm^{-1}. For laser irradiation, the cold window was rotated 90° and exposed to laser radiation entering the cryostat through a NaCl window mounted on an axis perpendicular to the spectrometer optical path (see Figure 1 in II). The grating-controlled CO_2 and CO laser beams used for excitation were expanded to the full size of the cold target.

Ozone-$^{16}O_3$ and ozone-$^{18}O_3$ were prepared in a thoroughly passivated stainless-steel vacuum system by the method described in I and then diluted with Ar, Kr, or N_2. In each case, the ozone was prepared from oxygen: $^{16}O_3$ from $^{16}O_2$ (Matheson, 99.99%) and $^{18}O_3$ from $^{18}O_2$ (Bio-Rad Laboratories, 99.13%). The NO (Matheson, 99.0%) was purified by two or three liquid-nitrogen trap-to-trap distil-

---

[1] M. A. A. Clyne, B. A. thrush, and R. P. Wayne, *Trans. Faraday Soc.*, **60**, 359 (1964); P. N. Clough and B. A. Thrush, *ibid.*, **63**, 915 (1967).

[2] P. N. Clough and B. A. Thrush, *Trans. Faraday Soc.*, **65**, 23 (1969).

[3] A. E. Redpath and M. Menzinger, *Can. J. Chem.*, **49**, 3063 (1971); *J. Chem. Phys.*, **62**, 1987 (1975).

[4] A. E. Redpath, M. Menzinger, and. T. Carrington, *Chem. Phys.*, **27**, 409 (1978).

[5] D. Van den Ende and S. Stolte, *Chem. Phys.*, **45**, 55 (1980).

[6] R. J. Gordon and M. C. Lin, *Chem. Phys. Lett.*, **22**, 262 (1973).

[7] M. J. Kurylo, W. Braun, A. Kaldor, S. M. Freund, and R. P. Wayne, *J. Photochem.*, **3**, 71 (1974).

[8] J. C. Stephenson and S. M. Freund, *J. Chem. Phys.*, **65**, 4303 (1976).

[9] S. L. Anderson, P. R. Brooks, J. D. Fite, and O. Van Nguyen, *J. Chem. Phys.*, **72**, 6521 (1980).

[10] D. Van den Ende and S. Stolte, *Chem. Phys. Lett.*, **76**, 13 (1980).

[11] G. R. Smith and W. A. Guillory, *Int. J. Chem. Kinet.*, **9**, 953 (1977).

[12] D. Lucas and G. C. Pimentel, *J. Phys. Chem.*, **83**, 2311 (1979).

[13] H. Frei, L. Fredin, and G. C. Pimentel, *J. Chem. Phys.*, **74**, 397 (1981).

0022-3654/81/2085-3355$01.25/0

TABLE I: Absorptions of NO and O_3 in Matrices $NO/O_3/M \approx 1:1:100$ at 12 K[a]

	frequency, cm^{-1}					
	$N^{16}O + {}^{16}O_3$				$N^{16}O + {}^{18}O_3$	
	isolated reactant					
mode[b]	N_2	Ar	Kr	$NO{\cdot}O_3$[e] N_2	isolated reactant N_2	$N^{16}O{\cdot}{}^{18}O_3N_2$
NO			1875.7			
		1876.7	1871.9			
	1874.9	1871.8	1869.1	1874.3	1874.9	1874.3
O_3 $3\nu_3(B_1)$		3046.6				
	3052.1	3041.3			2889.3	
$\nu_1 + \nu_3(B_1)$		2111.4	2103.3			
	2117.5	2108.3[d]	2099.8[d]		2002.2	
$\nu_1(a_1)$	1119.4	1103.4	1101.1		1046.4	
$\nu_3(b_1)$	1043.0	1040.9	1035.8		985.6	984.5
		1039.4[d]	1034.6[d]	1042.0		
	1040.9[c]	1037.9[c]	1033.3[c]			
$\nu_2(a_1)$	704.3	703.5	701.8		664.7	

[a] Absorptions of NO dimers as well as very weak bands due to other N_xO_y species were also observed. Their frequencies are summarized in Table 1 of I. [b] Cf. ref 17. [c] Dimers. [d] Second site. [e] No $NO{\cdot}O_3$ nearest-neighbor pair absorption could be observed in Ar or Kr matrices.

lations. Matrix gases argon (Matheson, 99.998%), krypton (Matheson, 99.995%), and nitrogen (Matheson, oxygen free) were used without further purification. The spectrum of the product aggregate $NO_2{\cdot}O_2$ was identified by codepositing O_2 (Matheson, 99.99%) and NO_2 (Matheson, 99.5%), from which residual NO had been removed by adding oxygen and condensing NO_2 at 77 K.

Results

In the experiments to be described, three matrix materials were used, N_2, Ar, and Kr. For each, a concentration study was carried out to determine the frequencies at which nearest-neighbor reactant pairs absorb and to identify the molecular aggregates obtained as reaction products. Then, the kinetics of the dark reactions in N_2 and in Ar were reinvestigated, and the study was extended to Kr matrices. Finally, the NO stretch of the $NO{\cdot}O_3$ pairs was excited with the CO laser to search for enhancement of the reaction rate through selective vibrational excitation.

Concentration Studies. The Ar and Kr matrix experiments for measuring the absorption frequencies of the $NO{\cdot}O_3$ pairs included concentrations $NO/O_3/Ar = 1:1:100$, 1:1:200, and 1:1:400. For N_2 matrix, $NO/O_3/N_2 = 1:1:100$, 1:2:100, and 1:4:100 were used. In addition, each reactant, NO and O_3, was studied alone in each matrix material at two different concentrations. For example, Figure 1 displays the dependence upon O_3 concentration of the absorption near 1875 cm^{-1} due to the NO stretch in $NO/O_3/N_2$ matrix samples. Table I summarizes the measured frequencies attributable to isolated reactants and those of $NO{\cdot}O_3$ pairs. Reactant pair absorptions could be identified only in N_2 matrices. Their frequencies were confirmed by the computer-calculated differences of the spectra before and after reaction.

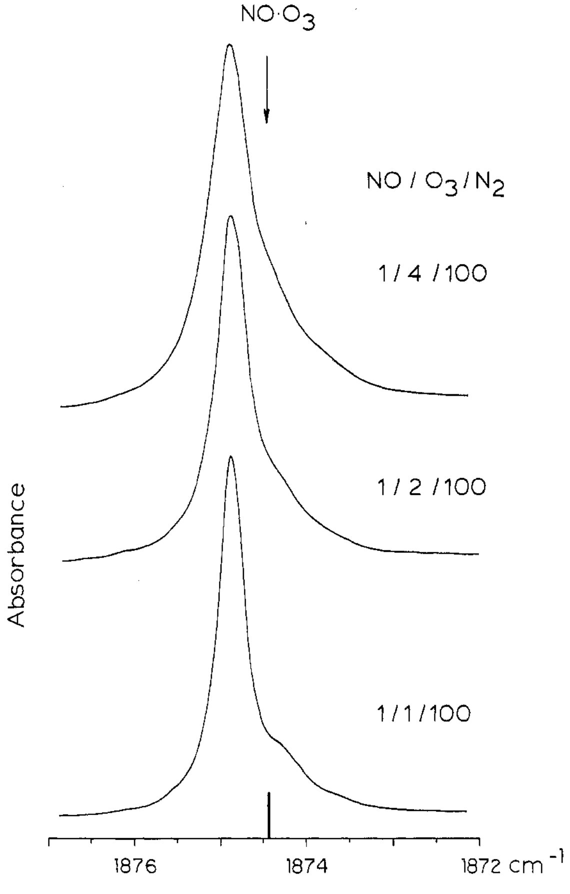

Figure 1. Concentration study for the NO + O_3 system in N_2 matrices at 12 K, ν(NO). Peak at 1874.9 cm^{-1} is assigned to isolated NO, shoulder at 1874.3 cm^{-1} to the $NO{\cdot}O_3$ nearest-neighbor pairs (marked by arrow). Marker on the abscissa scale indicates the position of the CO laser line at 1874.45 cm^{-1} used for irradiation.

Deposition experiments were conducted with samples of $NO_2/M = 1:400$ and with $NO_2/O_2/M = 1:1:200$ and 1:4:200 (M = N_2, Ar, Kr) to identify the characteristic frequencies of isolated NO_2 and of $NO_2{\cdot}O_2$ neighbor pairs. These frequencies coincide, within 0.1 cm^{-1}, with the absorptions observed in the same spectral regions from the various $NO/O_3/M$ samples immediately after deposition and then again after many hours had passed to permit growth of the product bands (see Table II). Figure 2, a and b, shows the types of product spectra observed with N_2 matrices. Figure 2a shows a triplet immediately after deposition with the central frequency at 1616.1 cm^{-1} appropriate to isolated NO_2. Figure 2b shows the spectrum of the same sample 33 h later. During the period, the two outermost features, at 1616.5 and 1615.2 cm^{-1}, have grown to dominate the spectrum (notice the ordinate scale change between 2a and 2b). These are the features in the $NO_2/O_2/N_2$ spectra which were assigned to $NO_2{\cdot}O_2$ pairs in two different sites (presumably, with different $NO_2{\cdot}O_2$ orientations). Plainly, each NO_2 is produced with an O_2 molecule in the same site, as is appropriate to reaction of one-to-one $NO{\cdot}O_3$ nearest-neighbor pairs.

Except for the 1616.1-cm^{-1} feature in N_2, all of the product absorptions in all three matrices were found at tunneling corrections needed in the analysis of the kinetics of the $(NO)_2 + O_2$ reaction at cryogenic temperatures.[11] Of course, the concept of low-temperature tunneling is not a new one, as was well reviewed by LeRoy and co-workers,[15] but the most convincing examples have involved H-atom movement. In fact, one of these systems, the H-atom abstraction by methyl radicals in methanol glasses, provides an interesting comparison to the present work. Hudson et al.[16] interpret the observed composite first-order kinetics to signify a "spectrum of reactivities" ... depending on the immediate environment of the methyl radicals" so that their derived rate constants "represents average values for all reaction orientations in the glassy matrix." We have been led to strinkingly similar interpretations.

Finally, we can add this reaction to the still short list of systems for which exciting one vibrational mode in an otherwise cold reactive pair can stimulate reaction (see references cited in II). Since this is a one-photon process, the photon energy, 5.35 kcal mol^{-1}, places an upper limit on the activation energy for the $NO-O_3$ reaction in the nitrogen matrix. How this excitation takes effect is ambiguous because of the orientational sensitivity displayed in the $NO \cdot O_3$ dark reaction. In any event, just as in the $C_2H_4 \cdot F_2$ case, the low quantum yield indicates effective relaxation by the matrix environment.

Acknowledgment. We gratefully acknowledge research support from the U.S. Air Force Office of Scientific Research under Grant No. AFOSR 78-3535. H. F. expresses appreciation to the Swiss National Science Foundation for fellowship support during this period (Grant No. 82.521.077).

---

(15) R. J. LeRoy, H. Murai, and F. Williams, *J. Am. Chem. Soc.*, **102**, 2325 (1980).

(16) R. L. Hudson, M. Shiotani, and F. Williams, *Chem. Phys. Lett.*, **48**, 193 (1977).

(17) L. Brewer and J. L. F. Wang, *J. Chem. Phys.*, **56**, 759 (1972).

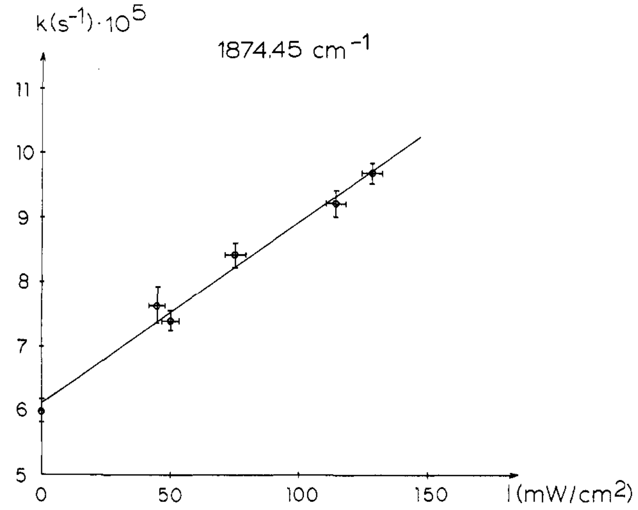

Figure 4. First-order rate constant of the NO + O_3 reaction in N_2 at 12 K as a function of CO laser power at 1874.45 cm^{-1}.

the dark-reaction rate-constant value, and its value increases monotonically with laser power. A plot of k vs. laser intensity is linear within our experimental uncertainty, as shown in Figure 4. Thus, the rate enhancement must be due to a single photon process. It is noteworthy that the ratio A_∞/A_0 is essentially constant (within 10%) in these experiment.

The CO_2 laser irradiation of isolated O_3 molecules offered an opportunity to investigate the possibility that these changes are in part due to bulk thermal effects. The last experiment listed in Table IV shows that, under 275 mW cm^{-2} CO_2 laser irradiation at 1043.16 cm^{-1}, the rate constant is enhanced over that of the dark reaction by only 19% whereas A_∞/A_0 is increased by a factor of 3. In view of the percentage absorption at the two frequencies, the CO_2 laser experiment deposits 4 times as much power as the CO experiment at 129 mW cm^{-2}. Plainly, there is a bulk thermal effect, but it is manifested primarily by an increase in the reservoir of reactive pairs (as indicated by A_∞/A_0) and by only a slight increase in k. We conclude that only a small fraction of the rate enhancement under CO irradiation can be due to bulk heating of the matrix.

Discussion

Dark Reaction. The absence of temperature dependence and the detection of an ^{18}O isotope effect point to a tunneling mechanism for the dark reaction. This conclusion provides a ready explanation for the existence of fast and slow reaction sites in an unannealed sample. Small orientational differences in the reaction complexes could cause small differences in the activation barrier. Because of the sensitivity of tunneling processes to barrier thickness, this would produce a considerable range of rate constants. At the same time, ambiguity is injected into any quantitative interpretation of the isotope effect. The rate behaviors of both fast and slow sites are represented in a single rate constant. Since the measurements extend over a fixed time period, the reaction rate of the light isotopes will tend to be more affected by the slower sites than will the rate of the heavy isotopes. Hence, the isotope effect will tend to be muted in the composite behavior.

This is readily shown through quantitative models. In the simplest picture, presented in I, an oxygen atom transfers through a barrier 2.3 kcal mol^{-1} in height (from the gas-phase value[1]) and with thickness chosen to fit the observed rate with normal isotopes (0.85 Å). Then the ^{18}O isotope can be expected to react tenfold slower. At another extreme, the entire NO molecule might tunnel through a 2.3 kcal mol^{-1} barrier to produce an NO_4 intermediate. The reduced mass for this model would lead to an ^{18}O isotope effect of only a twofold rate reduction (with a barrier thickness of 0.71 Å). With this range of expected isotope effect, it is easy to become convinced that roughly equal concentrations of fast and slow sites with tenfold different rate constants would display a measureable but quite modest ^{18}O isotope effect, as observed (~20%).

This deduction that the dark reaction is a tunneling process also provides an easy explanation for the observed sensitivity to the choice of matrix. Model calculations show that only a 2.5% change in the area under the barrier is needed to change the rate constant by a factor of 3.3, the difference between Kr and N_2 matrices. Such barrier changes could easily arise from the differences in site dimensions.

Laser-Enhanced Reaction. The data in Table IV and the plot of Figure 4 show conclusively that infrared excitation of the nitric oxide molecule in $NO{\cdot}O_3$ matrix pairs enhances the reaction rate constant k without noticeable increase in the reservoir of reactive pairs, as indicated by A_∞/A_0. Since the measured rate constants in Table III are average values over some spread of rate constants (fast and slow sites), the observed enhancement gives a lower limit on the enhancement for at least one of the sites.

A quantum yield can be obtained by assuming that the tunneling rate constant, k_t, and the photoinduced rate constant, k_{ph}, are simply additive.

$$k = k_t + k_{ph}$$

$$\phi = k_{ph}/I\epsilon = (1.0 \pm 0.8) \times 10^{-5}$$

I = number of incident CO laser photons/(s cm^2); ϵ = absorption coefficient per molecule of $NO{\cdot}O_3$ at 1874.2 cm^{-1} (estimated by assuming a statistical number of reactant pairs). The large uncertainty is due to the uncertainty in estimating the reactant $NO{\cdot}O_3$ concentration.

One interpretation of this rate enhancement is that vibrationally excited NO molecules react more rapidly than do ground-state molecules. However, since the enhanced rate constants are of the magnitude of k_{high} in the dark reaction, an alternate interpretation must be considered. It is also possible that NO ($v = 1$) molecules relax through excitation of librational modes that reorient the $NO{\cdot}O_3$ pairs, converting slow sites to fast sites.

Conclusions

The eluciation of the dark reaction as a tunneling process has interesting implications for the effect of the matrix on the activation energy. The gas-phase value, 2.3 kcal mol^{-1}, would suffice to suppress the thermal reaction of $NO(X^2\Pi_{1/2})$ with O_3 so that the much slower tunneling process can be observed. While our data indicate a considerable sensitivity of the rate constant to orientation in the reactant $NO{\cdot}O_3$ pair, this can be explained by only modest changes in a tunneling barrier with reasonable thickness and a height near the gas-phase value. Thus, we have no reason to postulate a large matrix effect on the NO + O_3 activation-energy barrier.

The identification of a bimolecular heavy-atom tunneling process is, of course, interesting in its own right since there are few well-established precedents. Goldanskii has postulated molecular tunneling in X-irradiation-induced cryogenic polymerization of formaldehyde.[14] Smith and Guillory consider the possibility that there are significant

---

(14) V. I. Goldanskii, *Science*, 182, 1344 (1973); *Annu. Rev. Phys. Chem.*, 27, 85 (1976).

TABLE III: First-Order Rate Constants for the Cryogenic Reaction NO + O_3 in Matrices $NO/O_3/M \approx 1:1:100$[a]

matrix	reaction	$NO_2 \cdot O_2$, cm^{-1}	T_{depn},[b] K	T_{expt},[b] K	k, h^{-1}
N_2	$N^{16}O + {}^{16}O_3$	1615.2	12	6	0.098 ± 0.003
	$N^{16}O + {}^{16}O_3$	1615.2	14	12	0.100 ± 0.001
	$N^{16}O + {}^{16}O_3$	1615.2	17	16	0.110 ± 0.002
	$N^{16}O + {}^{18}O_3$	1601.5	14	12	0.082 ± 0.001
Kr	$N^{16}O + {}^{16}O_3$	1607.2	12	12	0.335 ± 0.022

[a] All k values were determined from the growth over the first 12.5 h after the end of deposition. [b] T_{depn} = deposition temperature; T_{expt} = temperature at which the kinetics was measured after deposition.

TABLE IV: Dependence of the Rate Constant on the Laser Power at 1874.45 cm^{-1}, $NO/O_3/N_2 \approx 1:1:100$

I,[a] mW cm^{-2}	k,[b] h^{-1}	A_∞/A_0[c]	I,[a] mW cm^{-2}	k,[b] h^{-1}	A_∞/A_0[c]
0	0.216 ± 0.007	3.25	114	0.332 ± 0.009	3.03
45	0.275 ± 0.010	3.46	129	0.349 ± 0.006	3.48
51	0.266 ± 0.005	2.71	275[d]	0.257 ± 0.002	10.0
75	0.303 ± 0.007	3.67			

[a] TEM_{00}; 50% of the laser intensity was absorbed by NO. [b] All k values were derived from the growth of $NO_2 \cdot O_2$, 1615.2 cm^{-1}, over a period of 6 h after the beginning of laser irradiation. $T_{depn} = T_{expt}$ = 12 K for all experiments. [c] A_∞ = asymptotic absorbance of $NO_2 \cdot O_2$, 1615.2 cm^{-1}. A_0 = absorbance after deposition, just before the beginning of laser irradiation. [d] CO_2 laser irradiation at 1043.16 cm^{-1} with 99% absorption by isolated O_3 molecules.

found, however, to decrease as the temperature at which growth is permitted is raised; at 6 K it is ~4.4, and at 16 K it drops to ~1.2.

Figure 3a shows the simplest interpretation of our growth curves, a two-parameter (k, A_∞) least-squares fit of eq 1 to the data of an experiment in which the sample was both deposited and allowed to grow for 33 h at the same temperature, 12 K. Plainly the fit is not perfect during the first half of the experiment. In fact, this same systematic error pattern was observed in the best-fit representation of the data for every experiment of long duration at constant temperature. Thus, we see that with our more accurate photometry the rate behavior is not perfectly represented by eq 1. This can be displayed convincingly by fitting this two-parameter equation to the product absorbance data for increasing time periods. For the first 6 h, the best fit is obtained with a rate constant of 0.22 h^{-1} and $A_\infty = 0.14$ whereas, if the data up to 12 h are included, the best fit indicates $k = 0.13$ h^{-1} and $A_\infty = 0.17$. For the full 33 h of the experiment, the best-fit curve in Figure 3a corresponds to $k = 0.05$ h^{-1} and $A_\infty = 0.23$. This is the trend that would be expected, for example, if the growth is governed by two exponentials with quite different rate constants. In fact, the data shown in Figure 3a can be fitted within experimental uncertainty if we assume that there are two sites, each with first-order kinetics (eq 1) and with rate parameters $k_{fast} = 0.38$ h^{-1}, $A_\infty^{fast} - A_0^{fast} = 0.037$, and $k_{slow} = 0.034$ h^{-1}, $A_\infty^{slow} - A_0^{slow} = 0.171$, as pictured in Figure 3b. In this representation, these two rate constants can be attributed to two kinds of reactive sites, "fast" and "slow" sites.

This more detailed understanding of the kinetics immediately threw into doubt the interpretation of the temperature behavior recorded in I from which was deduced a small activation energy for local diffusion. Reanalysis of the earlier data revealed changes of A_∞ that suggested that there was a regeneration of fast sites during warming. This would, of course, vitiate a simple model of the observed growth rate immediately after warming. To escape this complexity, we conducted a series of three separate experiments in which for each experiment the growth was followed at a single temperature and for the same prescribed period, 12 h. Furthermore, to eliminate any possible generation of sites during the growth period (perhaps due to the reaction exothermity), the sample was deposited at a temperature a few degrees above that at which the growth was followed. The results are presented in Table III.

Since these experiments were all of the same duration, and only 12 h, they were analyzed in terms of eq 1 using only two parameters, A_∞ and k. Though the resulting k may represent the composite behavior of two or more reaction sites, it permits a meaningful comparison of the rate behavior at different temperatures. With this more controlled set of experiments, the apparent rate constants differ from those obtained earlier and now they show almost no change over the temperature range 6–16 K. This contradicts the results obtained in I that led to the activation-energy estimate. Now the earlier results can be seen to be an artifact of the experimental technique. Apparently fast reaction sites are generated during any temperature rise that exceeds the deposition temperature.

The effect of ^{18}O isotopic substitution was also repeated. Again, in contrast to the earlier work, the more controlled experiments and the improved accuracy showed that $^{18}O_3$ has a rate constant 20% below that of $^{16}O_3$.

Finally, Table III shows that the dark reaction in krypton matrix is threefold faster than the rate in nitrogen matrix.

Laser-Enhanced Reaction. In the presence of the dark reaction, the experiments in I failed to reveal any reaction rate enhancement due to infrared irradiation by the globar light source. With the present more accurate knowledge of the dark reaction, these experiments were repeated but using the 10^4 times more intense CO laser excitation source. The N_2 matrix was selected since its tunneling kinetics were best understood. In solid N_2, the $NO \cdot O_3$ pairs absorb at 1874.3 and 1042.0 cm^{-1}. The former frequency, the ozone-perturbed NO stretching mode, coincides closely with the $P_{10\rightarrow 9}(9)$ CO laser line at 1874.45 cm^{-1}. Unfortunately, the CO_2 laser only furnishes lines at 1043.16 cm^{-1} (which coincides with the absorption of isolated O_3 at 1043.0 cm^{-1}) and at 1041.28 cm^{-1}.

Taking advantage of the opportunity to excite the NO molecule in $NO \cdot O_3$ pairs, we conducted a series of experiments with the matrix sample exposed to 1874.45-cm^{-1} CO laser excitation at five different power levels. In each experiment, a first-order rate constant and A_∞ were obtained from a least-squares fit to the growth over a 6-h period of the $NO_2 \cdot O_2$ absorption at 1615.2 cm^{-1}. The values of k and A_∞/A_0 are presented in Table IV. The rate constant under irradiation at 129 mW cm^{-2} is 1.62 times

TABLE II: Absorptions of NO_2 Produced by the Reaction of NO with O_3 in Matrices $NO/O_3/M \approx 1:1:100$ at 12 K

	frequency, cm^{-1}							
	$N^{16}O + {}^{16}O_3$						$N^{16}O + {}^{18}O_3$	
	N_2		Ar		Kr		N_2	
mode	$NO_2{\cdot}O_2$	NO_2 isol	$NO_2{\cdot}O_2$	NO_2 isol	$NO_2{\cdot}O_2$	NO_2 isol	$N^{16}O^{18}O{\cdot}O_2$	$N^{16}O^{18}O$ isol
$\nu_1 + \nu_3(B_1)$	2910.8	2910.3[a]	2903.0	2904.2[a]	2895.9	2897.7[a]	2871.8	
			2902.2	2902.3[a]		2895.4[a]		
$\nu_3(b_1)$	1616.5	1616.1	1611.3	1611.8[a]	1607.2	1607.6[a]	1603.0	1602.4
	1615.2		1611.1	1610.8[a]		1606.5[a]	1601.5	
$\nu_2(a_1)$	750.7	750.4[a]	750.8	750.9[a]	749.6		738.9	

[a] Frequencies from matrices $NO_2/M \approx 1:400$. These absorptions could not be observed in matrices $NO/O_3/M$.

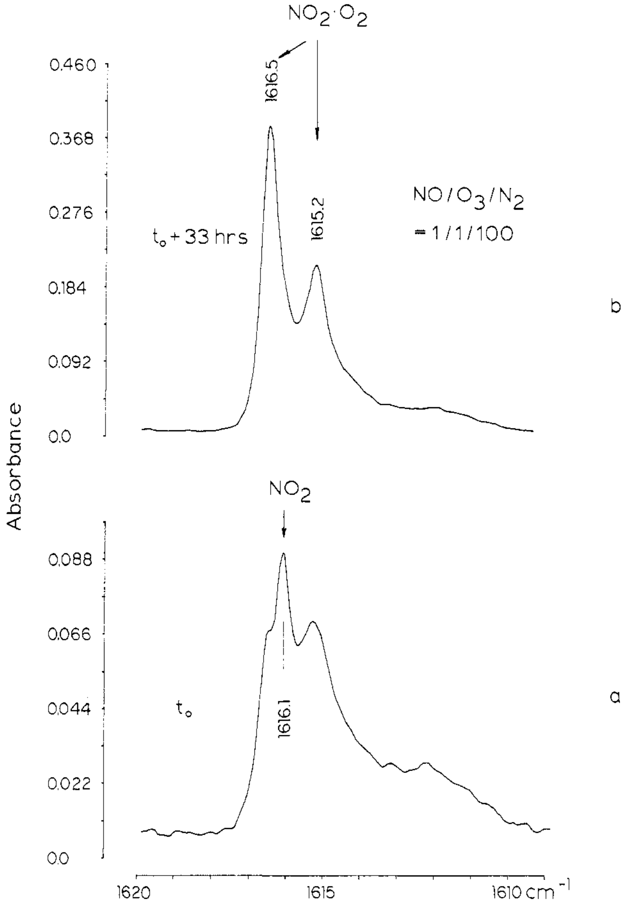

Figure 2. Growth of $\nu_3(NO_2)$ due to reaction of NO with O_3 in solid N_2 in the dark at 12 K: (a) spectrum after deposition; 1616.1 cm^{-1} is due to isolated NO_2 formed in gas-phase prereaction; 1616.5 and 1615.2 cm^{-1} are due to $NO_2{\cdot}O_2$ formed in matrix at different sites. (b) spectrum after 33 h; only the $NO_2{\cdot}O_2$ absorptions increased.

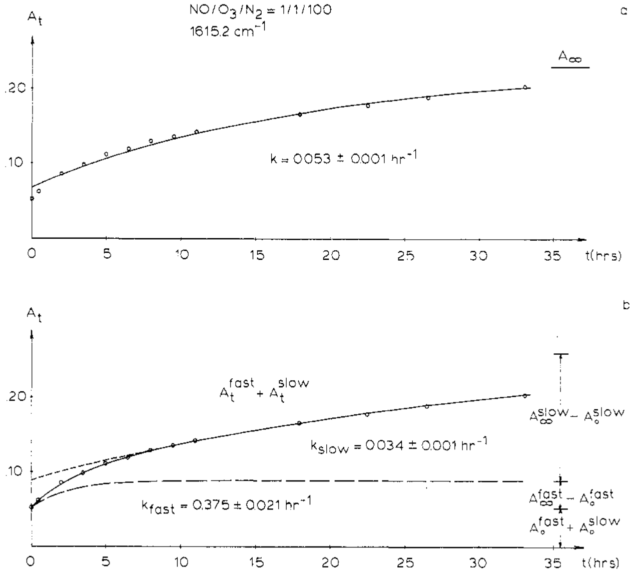

Figure 3. Growth of $NO_2{\cdot}O_2$ at 1615.2 cm^{-1} in solid N_2 in the dark at 12 K. End of deposition corresponds to $t = 0$. Each datum was obtained in a 10-min spectral scan. Upper plot: solid line is the best fit assuming a single first-order process. Lower plot: solid line is the best fit assuming two first-order processes as shown by dashed lines.

frequencies corresponding to $NO_2{\cdot}O_2$ pairs, both immediately after deposition and after growth.

Kinetic Treatment. If diffusion of the reactants cannot occur, either a dark reaction or a photochemical reaction between NO and O_3 nearest neighbors is expected to show kinetic growth appropriate to the first-order decomposition of a fixed reservoir of reactive pairs. This behavior was qualitatively noted in I, and the applicable rate equation was presented in II.

$$\ln \frac{A_\infty^{NO_2{\cdot}O_2} - A_t^{NO_2{\cdot}O_2}}{A_\infty^{NO_2{\cdot}O_2} - A_0^{NO_2{\cdot}O_2}} = -kt \qquad (1)$$

Peak absorbances were used since line widths remained constant within 3%. All absorbances refer to a particular feature attributed to $NO_2{\cdot}O_2$ product. $A^{NO_2{\cdot}O_2}$ represents the absorbance at completion of deposition (subscript 0), at time t (subscript t), or at time ∞ (subscript ∞).

For each kinetic study, the rate constant k and the absorbance A_∞, taken as parameters, were calculated from the growth of ν_3 of $NO_2{\cdot}O_2$ by seeking the linear regression that fitted eq 1 to the data with the best correlation coefficient.

Dark Reaction. In the earlier N_2 matrix study,[12] the following experimental results were presented: (1) Growth of NO_2 absorption at 1617 cm^{-1}, following a first-order rate constant of $(1.4 \pm 0.2) \times 10^{-5}\ s^{-1}$, was affected neither by several hours of exposure to Nernst glower irradiation ($\lambda > 1.8\ \mu m$) nor by removal of room-temperature background radiation with a 50° radiation shield. (2) When the matrix temperature was increased in steps from 12 to 20 K, the NO_2 growth curve steepened, and from the slopes an apparent activation energy of 106 cal mol^{-1} was obtained. (3) No isotope effect on the nitric oxide–ozone reaction rate was observed with either ${}^{18}O_3$ or ${}^{15}NO$.

The much higher resolution available to us in the present work provided both better accuracy in the optical density measurements and also the opportunity to measure separately the kinetic growth of each of the distinct sites (orientations) of $NO_2{\cdot}O_2$ product pairs (at 1615.2 and 1616.5 cm^{-1}, respectively). Within experimental uncertainty, the two features give identical rate constants. This outcome suggests that these two $NO_2{\cdot}O_2$ orientations are formed at a fixed ratio in the same process. This ratio is